J Mater Sci (2010) 45:1688–1694
DOI 10.1007/s10853-009-4158-4

Ultrasound assisted one pot synthesis of nano-sized CuO and its nanocomposite with poly(vinyl alcohol)

S. Gandhi · R. Hari Hara Subramani · T. Ramakrishnan · A. Sivabalan · V. Dhanalakshmi · M. R. Gopinathan Nair · R. Anbarasan

Received: 26 October 2009 / Accepted: 21 December 2009 / Published online: 5 January 2010

Abstract The ultrasound (US) assisted one pot method has used to synthesize CuO nanoparticles. The fourier transform infrared spectroscopy (FTIR) spectrum shows a characteristic peak of metal–oxygen bond at 535 cm^{-1}, which confirms the CuO formation. The high resolution transmission electron microscope (HRTEM) images of the synthesized nano-CuO confirms the size of nanorods with the length of approximately 25–30 nm, and its breadth is less than one nanometer. X-ray diffraction (XRD) pattern of CuO can be readily assigned to those of crystalline CuO, indicating the formation of single-phase CuO with monoclinic structure. The synthesized nano-CuO is mixed with poly(vinyl alcohol) (PVA) to prepare the PVA/CuO nanocomposite to improve the thermal stability of PVA. Their physico-chemical properties are examined by means of FTIR, XRD, differential scanning calorimetry, thermogravimetric analysis, HRTEM, and scanning electron microscope (SEM) techniques.

S. Gandhi · R. H. H. Subramani · T. Ramakrishnan · A. Sivabalan · V. Dhanalakshmi
Department of Polymer Technology, Kamaraj College of Engineering and Technology, Virdhunagar 626 001, Tamilnadu, India

M. R. G. Nair
School of Chemical Sciences, M.G. University, Kottayam 686 560, Kerala, India

R. Anbarasan (✉)
MEMS Thermal Control Lab, Department of Mechanical Engineering, National Taiwan University, Taipei 10617, Taiwan, ROC
e-mail: anbu_may3@yahoo.co.in

Introduction

Studies on 1D nanomaterials are of great interest due to their unique physical, chemical, optical, and mechanical properties [1, 2]. Among the 1D nanomaterials, primarily we are very much interested in CuO because of its surface catalytic effect [3] and chelating effect, whereas the other conventional metal oxides are having only the surface catalytic effect, which leads to oxidation reaction. The oxidized products show unwanted properties like depression in thermal stability. The combination behaviors of surface catalytic effect and complex formation effect of CuO urged us to do the present investigation. CuO is a p-type semi conductor with a band gap of 1.2 eV. Various methods are available for the synthesis of such a useful material. Hydrothermal synthesis of shuttle like CuO was synthesized and characterized by Chen et al. [4]. Dodecyl sulfate intercalated CuO was synthesized and characterized by XRD, thermogravimetric analysis (TGA), TEM, and SEM techniques [5]. $Cu(OH)_2$ template synthesis of CuO nanowire was reported in the literature [6]. Hong et al. [7] synthesized the CuO nanoparticle by alcohothermal approach. Solution phase synthesis of CuO nanorod [8], hydrothermal synthesis of CuO microsphere [9], one step solid state CuO nanopowder [10], CuO nanocrystals with different shapes [11], microwave synthesis of CuO nanoflower [12], CuO synthesis by electrochemical method [13], and pre-cursor based route [14] reports are available in the literature. The other authors also reported about the synthesis and characterizations of CuO nanoparticle by different approaches [15–22]. By thorough literature survey, we found that very few reports are available regarding the synthesis of CuO by ultrasound (US) assisted one pot method. Hence, in the present investigation, we took this job as a challenge and synthesized the CuO nanoparticle by

the US assisted one pot method and made nanocomposite with poly(vinyl alcohol) (PVA), a bio-degradable polymer, to boost up the thermal stability of PVA for certain end use application. The role of nano-sized CuO on the PVA structure was quantitatively estimated through FTIR spectrometer for the first time.

Experimental

Materials

Copper acetate monohydrate (CA) and Hydrochloric acid were purchased from Ottochemi, India. The PVA used in this work was obtained in powder form from S.D. fine chemicals, India with the weight average molecular weight of 1,25,000 (85% hydrolyzed). Brydson Ultrasonicator, USA with the frequency of 40 kHz was used for US generation purpose. Double-distilled (DD) water was used for the preparation of reactant solutions.

Synthesis of nano-sized CuO

Nanostructured CuO was synthesized by the one pot sonochemical method. In a typical experimental procedure: 5 g of CA was dissolved in 100 mL of deionized water in a beaker, which was placed in an ice bath, and 10 mL of conc. HCl was poured drop wise in this solution while stirring it continuously. The stirring was continued for 10 min. Subsequently, the resultant solution was first sonicated at 40 kHz for 30 min in an ice bath, then at room temperature while the solution temperature was raised to 80 °C and heated the solution to 130 °C with simultaneous ultrasonication. The precipitate was filtered and washed with methanol several times to remove the ionic impurities and finally dried under vacuum for 48 h at room temperature.

Preparation of PVA/CuO nanocomposite film

Poly(vinyl alcohol) with molecular weight of 1, 25,000 (85% hydrolyzed) was used as basic polymeric material in this work. PVA films were prepared by using a casting technique. PVA solution was prepared by dissolving 1.0 g PVA in DD water and maintained for 24 h at room temperature to swell. The solution was then warmed up to 60 °C and thoroughly stirred, using a magnetic stirrer for 4 h until the polymer produced a clear solution. The solution was poured onto polyimide film to get a film with uniform thickness. Homogeneous films were obtained after drying in an air oven for 48 h at 40 °C and PVA films filled with as-synthesized nano-sized CuO mass fractions 0, 2, 4, 6, 8, and 10% were also prepared. The prepared films were free from air bubbles and with uniformly dispersed CuO nanoparticles. The thicknesses of the produced films were in the range of 0.1–0.21 mm and cut into pieces suitable for measurements.

Characterizations

The FTIR spectrum was recorded using a Shimadzu FTIR-8400 S model instrument. The relative intensity (RI) of peaks was determined after proper baseline correction by using FTIR software as follows:

$$\text{RI of C} = \text{O} \;=\; \text{RI}_{[\text{C=O/CH}]} = A_{1733}/A_{844}, \tag{1}$$

$$\text{RI of C} = \text{C} \;=\; \text{RI}_{[\text{C=C/CH}]} = A_{1661}/A_{844}. \tag{2}$$

XRD of the samples were recorded with a help of Philips PW 1050/80 diffractometer with Ni-filtered CuKα radiation generated 30 kV and 15 mA. Thermal analyses were performed by differential scanning calorimetry (DSC) using Shimadzu DSC-50 under nitrogen atmosphere at the heating rate of 10 °C/min in nitrogen atmosphere. The thermal stability of nanocomposite was examined by TGA instrument by using STA 1500 PL Thermal Sciences instrument. Synthesized nanomaterial topography and size were observed by HRTEM on a JEM-200 CX transmission electron microscope and cross-section of morphology of the films was studied using SEM, S-2830N Hitachi, Japan instrument.

Results and discussion

This section is broadly classified into (i) characterizations of synthesized nano-CuO and (ii) characterizations of PVA/CuO nanocomposites.

Characterizations of synthesized nano-sized CuO

FTIR study

The FTIR spectrum of pristine CuO is given in Fig. 1. The metal–oxygen (M–O) stretching was observed at 650 cm^{-1}. A broad band in the range of 3,600–3,100 cm^{-1} is due to the OH stretching of water molecules chemically associated with CuO. Recently, Parveen et al. [23] explained the M–O stretching in $Cu(OH)_2$. The present investigation is in accordance with their report.

XRD analysis

The crystalline nature of synthesized nano-CuO was observed by the various sharp crystalline peaks in the XRD pattern of nano-CuO. XRD pattern of CuO (Fig. 2) was

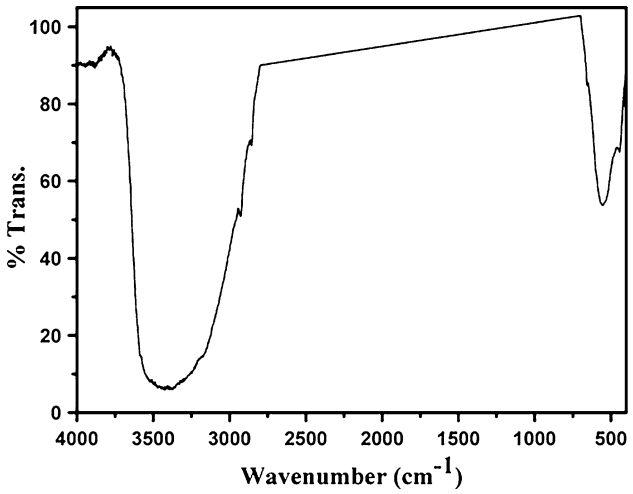

Fig. 1 FTIR spectrum of pristine CuO

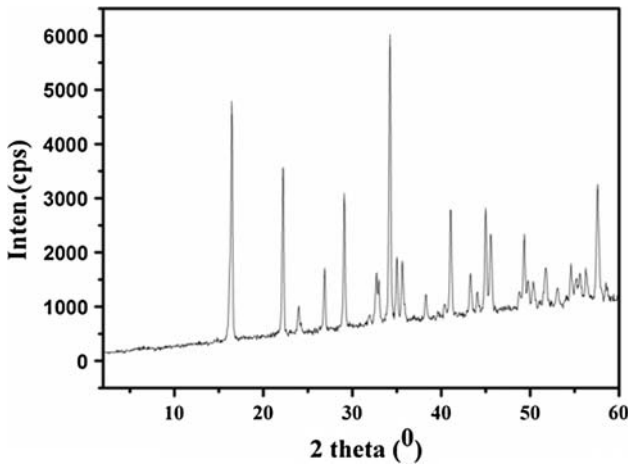

Fig. 2 XRD pattern of pristine CuO

compared with the data of the JCPDS file no. 5-0661 and all peaks can be readily assigned to those of crystalline CuO, indicating the formation of single-phase CuO with monoclinic structure [24].

HRTEM images

The HRTEM images (Fig. 3a) of the CuO nanorods revealed that these materials have a relatively straight rod like shape and smooth surfaces. It can also be seen that the nanorods are having the length of approximately 25–30 nm, and its breadth is less than 1 nm. The visible fringes illustrate that the nanorod is crystalline. Figure 3b, c indicate the agglomerated rod-shaped CuO. The SAED pattern (Fig. 3d) exhibits bright dots rather than rings, indicating that it consists of CuO nanocrystals with randomly oriented crystallographic planes [24]. By using the US assisted one pot method, we produced a typical nano-sized CuO when compared with the literature value [6].

Characterizations of PVA/CuO nanocomposites

FTIR report

The FTIR spectra of pristine and CuO filled PVA is shown in Fig. 4. The important peaks are characterized below: a strong broad band at 3,427 cm^{-1} is assigned to O–H stretching vibration of hydroxyl groups of PVA. The band corresponding to C–H asymmetric stretching vibration occurs at 2,925 cm^{-1} and C–H symmetric stretching vibration at 2,861 cm^{-1}. A peak at 1733 corresponds to C=O stretching vibration and 1,640 cm^{-1} is corresponding to a C=C group in PVA backbone and can be explained on the basis of intra/inter molecular hydrogen bonding with the neighboring OH groups. A sharp band at 1,087 cm^{-1} corresponds to C–O–C stretching of acetyl group present on the PVA back bone. The corresponding bending, wagging of CH_2 vibrations are at 1,437 and 1,379 cm^{-1}, respectively, and the C–H wagging at 1,247 cm^{-1}. The incorporation nano-sized CuO in PVA caused the slight changes in the intensities of absorption bands at 1,733 and 1,640 cm^{-1} as well as the formation of new absorption bands in the range of 1,000–600 cm^{-1}. Peak around 1,000–600 cm^{-1} is attributed to the metal–oxygen stretching of CuO [25]. This confirmed the presence of nano-sized CuO particles present in the PVA matrix. Peaks at 1,733 and 1,640 cm^{-1} were assigned to C=O stretching, and C=C group in PVA backbone were increased while increasing the wt% loading of nano-sized CuO. The added nano-CuO was acting as a catalyst for the oxidation process in the PVA backbone, which was confirmed in the FTIR–RI analysis.

Surface catalytic effect of CuO on the PVA matrix

The added nano-sized CuO altered the structure of PVA in two ways. First, it activated the conversion of secondary alcoholic group into a keto group via thermolytic oxidation reaction. Second, it boosted the formation of double bond along the PVA chains through its surface catalytic effect. The C=C might be formed at the PVA chain end or in the middle of PVA chain. Figure 5a shows a plot of log(wt% of CuO) versus $\log(RI_{[C=O/CH]})$ and Fig. 5b shows a plot of log(wt% of CuO) versus $\log(RI_{[C=C/CH]})$. The added nano-CuO converted the secondary alcoholic group into keto and oxidized the vinyl group into alkenes in the PVA backbone. The order of reaction for the above mentioned plots were determined as 1.41 and 1.56, respectively, for carbonyl and alkene formation reactions. It means that 1.5 mol of nano-sized CuO is required to convert 1 mole of secondary alcoholic group into a keto group and 1 mole of alkene group. This confirmed the catalytic effect of nano-CuO in

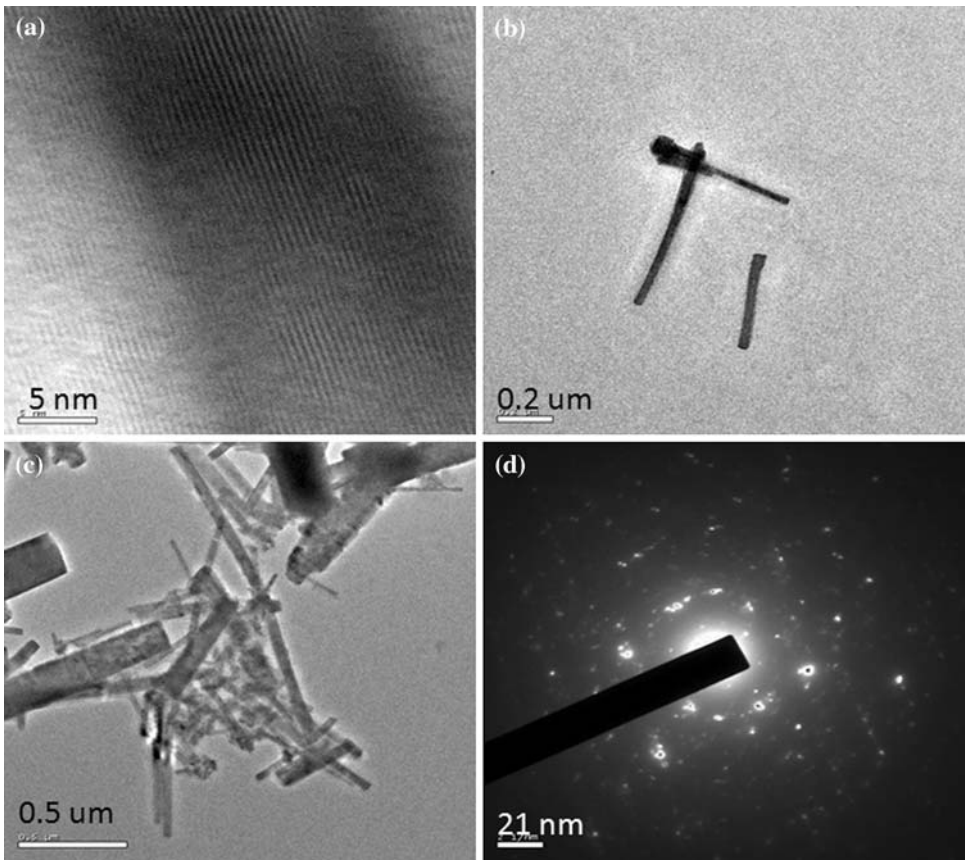

Fig. 3 **a–d** HRTEM images of CuO nanorods

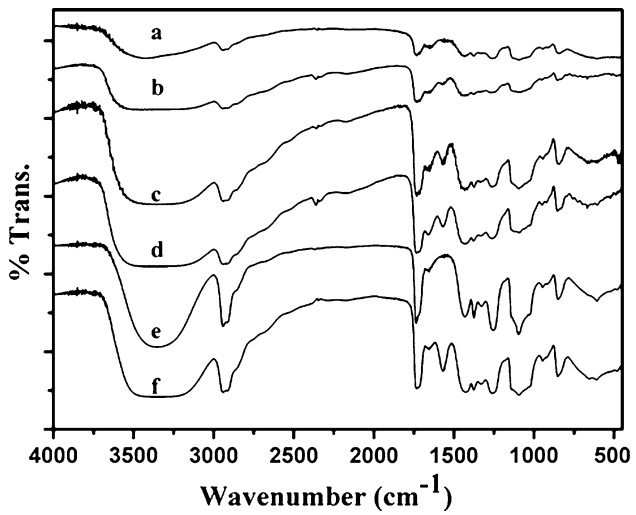

Fig. 4 FTIR spectrum of PVA loaded with CuO at *a* 0 wt%, *b* 1 wt%, *c* 3 wt%, *d* 5 wt%, *e* 7 wt%, *f* 9 wt%

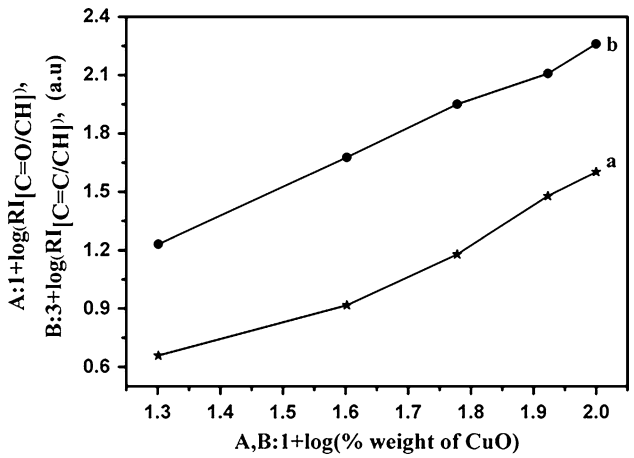

Fig. 5 Effect of (wt% of CuO) on the *a* $RI_{[C=O/CH]}$, *b* $RI_{[C=C/CH]}$

the oxidative degradation reaction in PVA backbone. This is in accordance with Parveen's report [15].

XRD studies of polymer nanocomposite

Figure 6 reveals the XRD scans of pristine PVA and PVA containing different wt% loading of CuO. It is obvious that there is no significant effect on the general shape of the XRD pattern. The observed spectra characterized a semi crystalline polymer possessing, a clear crystalline peak for all studied samples. A peak at $2\theta = 20°$ is corresponding to (101) crystal plane for PVA, which indicates the semi crystalline nature of PVA. The crystalline nature of PVA results from the strong intermolecular interaction between PVA chains. The intensity of the PVA main diffraction peak (101) is further decreased due to the host effect of

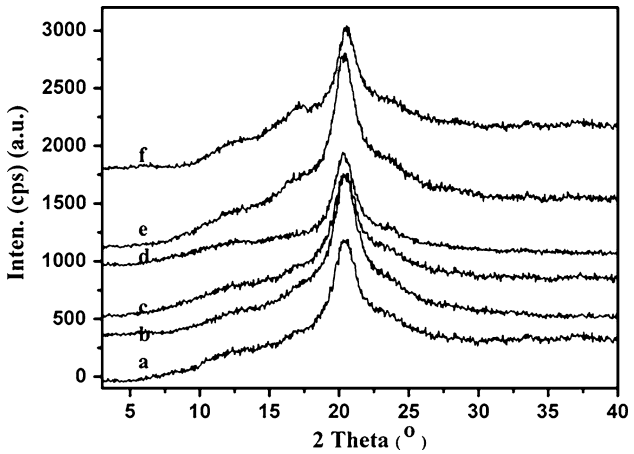

Fig. 6 XRD of PVA loaded with CuO at *a* 0 wt%, *b* 1 wt%, *c* 3 wt%, *d* 5 wt%, *e* 7 wt%, *f* 9 wt%

nano-CuO. This is because of interactions between PVA and mixed CuO lead to a decrease in the intermolecular interaction between PVA chains and thus the lower the crystalline degree [26].

TGA analysis

Thermal stability of the polymer/nanocomposites was evaluated by TGA method. The TGA of pristine and various wt% of CuO loaded PVA is represented in Fig. 7. The thermal degradation of the pristine PVA has two-step degradation processes. In the first minor weight loss step, the elimination of moisture and physisorbed H_2O molecules occurred, and in the second weight loss step, PVA main chain degradation occurred. Rachna and Rao [27] reported about the thermal degradation of PVA. Our reports coincided with them. Similarly, the thermal degradation of PVA/CuO nanocomposite showed a two-step degradation process. The thermogravimetric curve of the PVA/CuO nanocomposite is situated at a higher temperature than that of the pristine PVA. The introduction of CuO nanoparticles on PVA matrix greatly improved the thermal resistance. Therefore, the PVA/CuO nanocomposite is thermally more stable than the pristine PVA. The increase in thermal stability is due to the surface catalytic effect and complex formation effect of CuO nanoparticles. Because the surface catalytic effect of CuO makes the PVA backbone more rigid via creating C=C double bond. The Cu^{2+} ions of CuO involved in the complex formation with the OH groups of PVA. Hence, the combined effect of surface catalytic effect and chelating effect increased the thermal stability of PVA. Peng and Kong [28] reported the similar result for filled SiO_2–PVA nanocomposite system. When compared with the literature, the present system exhibited somewhat improved thermal stability of PVA.

DSC analysis

Figure 8a shows the DSC of pristine PVA with the $T_{d.w}$, T_{α}, and T_m values of 111.5, 195.6, and 328.3 °C, respectively. On making nanocomposite with CuO, the T_m value of PVA was drastically reduced due to the hydrolytic oxidation and oxidative degradation reactions. The 2 wt% CuO loaded PVA exhibited the T_m value at 259.2 °C (Fig. 8b). While increasing the wt% loading of CuO (Fig. 8c–f), the T_m value of PVA was slightly increased up to 8 wt% loading. This explained the complex forming behavior of metal ions with PVA. Such a complex formation of metal ions with PVA was reported by Gaffer et al. [29]. The important point noted here is while increasing the wt% loading of CuO, the second T_m was observed at 242.3 °C. This is due to the T_m of PVA chains with different molecular weight.

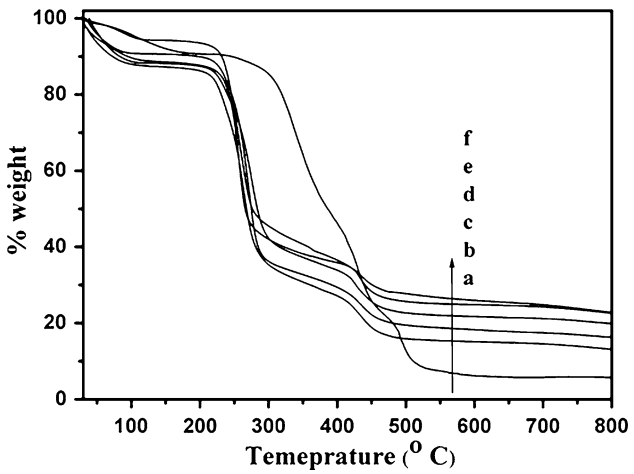

Fig. 7 TGA of PVA loaded with CuO at *a* 0 wt%, *b* 1 wt%, *c* 3 wt%, *d* 5 wt%, *e* 7 wt%, *f* 9 wt%

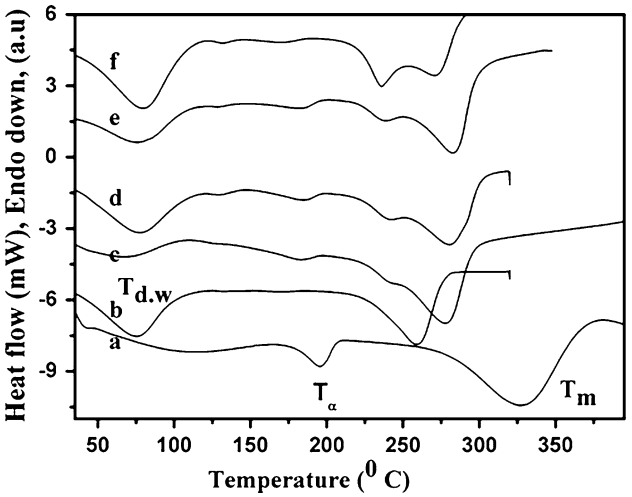

Fig. 8 DSC of PVA loaded with CuO at *a* 0 wt%, *b* 1 wt%, *c* 3 wt%, *d* 5 wt%, *e* 7 wt%, *f* 9 wt%

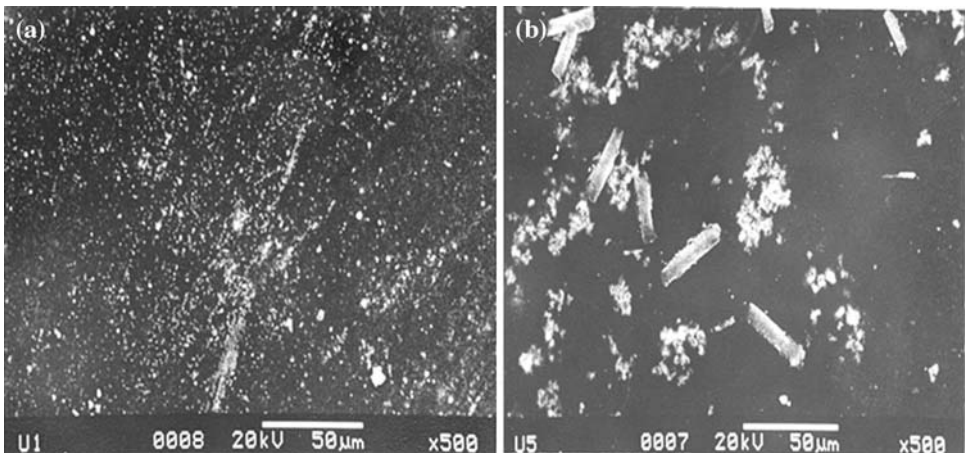

Fig. 9 SEM image of **a** 2 wt% Cuo loaded PVA, **b** 10 wt% CuO loaded PVA

Different molecular weight of PVA was obtained as a result of C=C formation at the chain end. Formation of terminal double bond was accelerated with the surface catalytic effect of CuO. At 10 wt% CuO loaded in PVA matrix, the second T_m has been clearly observed with the reduction in first T_m value. This clearly explained that at higher wt% loading of CuO, due to the surface catalytic effect, the formation of terminal C=C was accelerated, which can be further supported with the order of $RI_{[C=C/CH]}$. The DSC study revealed that at lower wt% loading of CuO, the complex formation and surface catalytic effects were competitive one, whereas at higher wt% loading of CuO, the later effect was a dominant one due to the active surface area with nano size. This concluded that at higher wt% loading of CuO, the catalytic effect is dominating than the chelating effect [30]. Moreover, at higher wt% loading of CuO, agglomeration occurred and produced the depressed product.

SEM images

The morphology of 2 and 10 wt% nano-CuO filled PVA were studied using SEM image and shown in Fig. 9. The synthesized nano-CuO particles are uniformly dispersed in the lower wt%, i.e., 2 wt% (Fig. 9a). The morphology of higher wt% (10 wt%, Fig. 9b) of CuO loaded PVA showed the agglomeration of CuO nanoparticles when increasing its content. This confirms the higher concentration of nanofiller leads to the agglomeration in PVA matrix.

Conclusions

The CuO nanorods with ca. less than 1 nm in diameter and 25–30 nm in length were synthesized via a one pot sonochemical method. The formation of CuO was confirmed by the metal–oxygen peak at 650 cm^{-1}. The catalytic effect of synthesized CuO, involvement in simultaneous oxidation, and thermal degradation processes on PVA in the order of 1.5 was confirmed by FTIR-RI and XRD revealed that the filled CuO lead to the lower crystalline degree of PVA matrix due to decrease in the intermolecular interaction between PVA chains. The introduction of CuO nanoparticles in PVA matrix greatly improved the thermal properties, which were confirmed by TGA and DSC analysis. Formation of double bond in PVA backbone was accelerated with the surface catalytic effect of CuO. The higher wt% loading of CuO nanoparticles onto PVA matrix led to agglomeration observed in SEM images.

References

1. Duan XF, Huang Y, Agarwal R, Lieber CM (2003) Nature 421:241. doi:10.1038/nature01353
2. Zhu HW, Xu CL, Wu DH, Ajayan PM (2002) Science 296:884. doi:10.1038/nature00767
3. Xu Z, Qian Z, Hattori H (1991) Bull Chem Soc Jpn 64:1658
4. Chen D, Shen G, Tang K, Qian Y (2003) J Cryst Growth 254:225. doi:10.1016/S0022-0248(03)01170
5. Huk YD, Kweon SS (2005) Bull Korean Chem Soc 26:2054
6. Wang WZ, Vargheese OK, Ruan C, Grimes CA (2003) J Mater Res 18:2756
7. Hong ZS, Cao Y, Deng JF (2002) Mater Lett 52:34
8. Liu Q, Liang Y, Liu H, Hong J, Xu Z (2006) Mater Chem Phys 98:519. doi:10.1016/j.matchemphys.2005.09.073
9. Yu H, Yu J, Liu S, Mann S (2007) Chem Mater 19:4327. doi:10.1021/cm070386d
10. Dianzeng J, Jianqun Y, Xi X (1998) Chin Sci Bull 43:571
11. Zhou K, Wang R, Xu B, Li Y (2006) Nanotechnology 17:3939. doi:10.1088/0957-4484/17/15/055
12. Volanti DP, Keyson D, Simoes AZ, Souza AG (2008) J Alloys Compd 459:537. doi:10.1016/jalloycom.2007.05.023
13. Stankovic ZD, Krcobic S, Wregg AA (1999) J Appl Electrochem 29:81
14. Li JY, Xiong S, Xi B, Qian YT (2009) Cryst Growth Des 9:4108. doi:10.1021/cg900346p
15. Xu CH, Woo CH, Qshi S (2004) Superlattice Microstruct 36:31. doi:10.1016/j.spmi.2004.08.021
16. Fan H, Yang L, Hua W, Xie S, Zou B (2004) Nanotechnology 15:37. doi:10.1088/0957-4484(04)61337-7

17. Savoicka K, Karadge M, Prasad AK, Gouma PI (2004) Microsc Microanal 10:360. doi:10.1017/S1431927604886033
18. Dar MA, Ahsanulhaq Q, Kim KS, Shim HS (2009) Appl Surf Sci 255:6279. doi:10.1016/j.apsusc.2009.02.002
19. Wu H, Lin D, Ran W (2006) Appl Phys Lett 89:133125-1. doi:10.1063/1.2355474
20. Zhang K, Rossi C, Yves J, Chang C (2007) Nanotechnology 18:275607-1. doi:10.1088/0957-4484/18/27/275607
21. Li W, Bin Z, Xian CL, Jun XW (2007) Sci China Ser B Chem 50:63. doi:10.1007/S11426-007-0016-x
22. Du GH, van Tendeloo G (2004) Chem Phys Lett 393:64. doi:10.1016/j.cplett.2004.06.017
23. Parveen MF, Umapathy S, Dhanalakshmi V, Anbarasan R (2009) Nano 4:147. doi:10.1142/S17932920009001654
24. Wang W, Liu Z, Liu Y, Xu C, Zheng C, Wang G (2003) Appl Phys A 76:417. doi:10.10107/s00339-002-1514-5
25. Abdelaziz M, Abdelrazek EM (2007) Physica B 390:1. doi:10.1016/jphysb.2006.07.067
26. Yu YH, Lin CY, Yeh JM, Lin WH (2003) Polymer 44:2553. doi:10.1016/S0032-3861(03)00106-x
27. Rachna M, Rao KJ (1999) Eur Polym J 35:1883
28. Peng Z, Kong LX (2007) Polym Degrad Stab 92:207. doi:10.1016/j.polymdegradstab.2006.11.008
29. Gaffer SA, Abd El-Kader FH, Rizk MS (1994) Phys Scr 49:366
30. Parveen MF, Umapathy S, Dhanalakshmi V, Anbarasan R (2009) J Mater Sci 44:5852. doi:10.1007/s10853-009-3826-8